EXPERIMENTAL STURY OF PARTICLES MIXING BEHAVIOR IN A MODIFIED INTERNALLY CIRCULATING FLUIDIZED BED

Mengxi Liu*, Zhenliang Meng, Yiping Fan, Chunxi Lu

State Key Laboratory of Heavy Oil Processing, Faculty of Chemical Engineering, China University of Petroleum Beijing, Fuxue Road, Changping, Beijing 102249, PR China

*Email: mengxiliu@sina.com

Abstract – Solid mixing has an important effect on heat transfer, reaction rate and product quality. In this paper, a modified internally circulating fluidized bed, consisting of a draft tube with four symmetrical rectangular slots, was proposed to enhance the particles mixing, especially in the radial direction. The mixing characteristics in the reactor under different operating conditions were investigated. The results show that in the draft tube, the degree of particles mixing in the center was better than near the wall and the horizontal particles flow at the slots was benefit for the particles radial mixing. The mixing index was more than 0.97 in the draft tube. The mixing performance was slightly changed with mass flux.

1. Introduction

The fluidized bed (FB) is widely used in material synthesis, petrochemical and biochemical processes. Extensive studies have been conducted on hydrodynamics, mass and heat transfer and reaction performance, but few of them addressed on particle mixing behavior in the fluidized beds. Westphalen and Glicksman (1995) measured radial particle mixing in a circulating fluidized bed, and discovered that the radial diffusion coefficient was 0.0001 m^2/s at the top of the riser. Meanwhile, at the bottom of the riser, the radial particle mixing was more vigorous. Fushimi et al. (2012) observed the particle mixing behaviors of a downer using thermal particle tracking technology, and found that the nozzle arrangement has a great influence on the mixing performance, and a tangential opening is more conducive for particle mixing than a common middle opening. Yang et al. (2014) investigated solid mixing characteristics in the bubbling fluidized bed using CFD simulation. These results showed that the dead zone and the mixing rate in the horizontal direction are the two common problems to solve.

By mounting vertical baffles or draft tube in a free bed, the internally circulating fluidized bed (ICFB) realizes the orderly particle circulation in the reactor. The multiple particles cycles significantly promote particles mixing, especially radial particle mixing in the reactor. Simultaneously, the forced particle circulation effectively reduces the dead zone. Fang et al. (2013) studied the solid mixing characteristics in an ICFB and compared it with the convectional FB. They found that the special circulation flow of solid greatly enhanced horizontal mixing and the ICFB exhibited better solid mixing ability than the conventional FB. Liu et al. (2015) proposed a new type of particle mixer, consisting of a pre-mixing section, along with a modified ICFB mixer section. It was found that the mixing index in the pre-mixing section could reach 0.7 and the final mixing index could reach 0.95. Compared with the convectional FB, the ICFB had a better particles mixing performance. However, the capacity of the radial particles mixing in the ICFB still needs to be further improved. In the present work, a modified internally circulating fluidized bed (MICFB) was proposed on the basis of the research of Liu et al. (2015). The mixing behavior of cold and hot particles in the reactor was studied.

2. Experiment

2.1. The novel gas-solid air loop reactor

As shown in Fig. 1, the mixer consists of a pre-mixing section and an ICFB mixer section. A draft tube is coaxially mounted in the reactor, and four rectangular slots symmetrically opened on the draft tube, aiming to improving radial particles mixing. The MICFB is divided into five zones, i.e. bottom zone, draft tube zone, slot zone, gas-solid separation zone and annulus zone. Above the draft tube, there is a perforated plate. Cold and hot particles flow into this zone and pre-mix, then, flow downward into the MICFB section through the central downcomer. The configuration of the MICFB and measurement points are shown in Fig. 1.

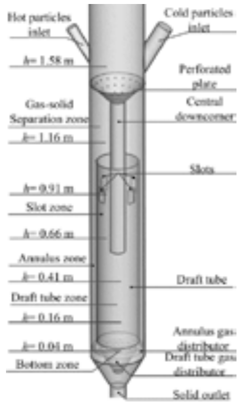

Fig. 1. Schematic diagram of gas-solid air loop reactor

2.2. Apparatus and experimental material

The schematic diagram of experimental apparatus is shown in Fig. 2. It mainly includes a particles heater, the MICFB section, the riser, and a bubbling fluidized bed. Particle is FCC catalyst (ρ_p= 1498 kg/m^3) with an average diameter of 79 μm.

As shown in Fig. 2, the cold particles are fluidized by air in the bubbling fluidized bed, and are introduced into the MICFB. The hot particles are injected into the MICFB from the particle heater by compressed air and mixed with the cold particles in the MICFB. Then the mixed particles flow out the MICFB and into the bottom of the riser. At the end of the riser, particles are separated via cyclones and return to the bubbling fluidized bed.

The superficial gas velocity, u_{gd}, varies from 0.3 to 0.5 m/s in the draft tube and remains 0.1 m/s in the annulus. The total solid mass flux is 68.9-89.56 kg/ (m^{2}s), based on the cross-sectional area of the MICFB. The mass flux ratios of the hot particles to the cold particles in the experiments range from 2.25 to 9.

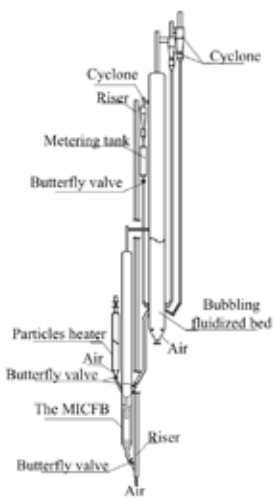

Fig. 2. Schematic diagram of experimental apparatus

2.3. Thermal tracer technology

Fig. 3 shows the schematic diagram of the thermal probe, which has a diameter of 6 mm and consists of epoxy resin and a stainless steel tube. The measurement accuracy of the surface thermistor sensors within the experimental scope is 0.2℃. The output signals from the thermocouples are registered at a sampling frequency of 10 Hz and with a sampling time of 500 s.

In each test, 45 kg FCC particles were heated to 140℃ in the particles heater, and then injected into the MICFB under compressed air. By measuring the temperature at different radial and angular points, the particles mixing degree was quantitatively analyzed and evaluated.

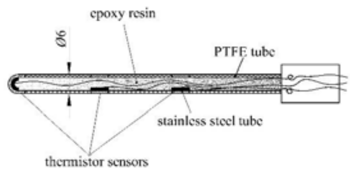

Fig. 3. Schematic diagram of thermal probe

3. Result and discussion

3.1 Temperature distribution in different zones

Fig. 4 illustrates the temperature distribution in the pre-mixing section. As shown in Fig.1, hot particles were induced on the axial of θ=180°. On this side, the temperature was relatively high in the section of r/R=0.42 to 0.65, suggesting that hot particles mainly fall into this section. Furthermore, the temperature on the axial of θ=180° was considerably higher than on other axial, which indicated that the mixing of hot and cold particles are poor across the section.

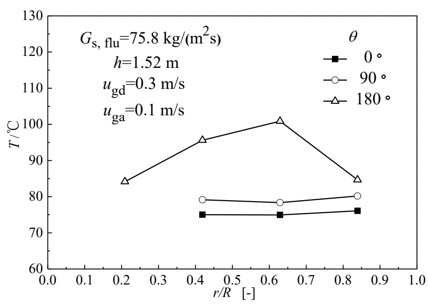

Fig. 4. The temperature distribution in pre-mixed zone

Fig. 5 illustrates the temperature distribution in the draft tube zone. In the draft tube zone, the hot particles flowed out of the central downcomer and mixed with the cold particles in the draft tube. This counter current contact of downwards flowing hot particles and upwards flowing cold particles led to a strong mixing section. It can be seen that in the central area ($0<r/R<0.5$), the temperature was slightly higher than that near the wall. This indicated that hot particles out of the central downcomer migrated to the vicinity of the wall, and suggested a strong radial mixing of particles.

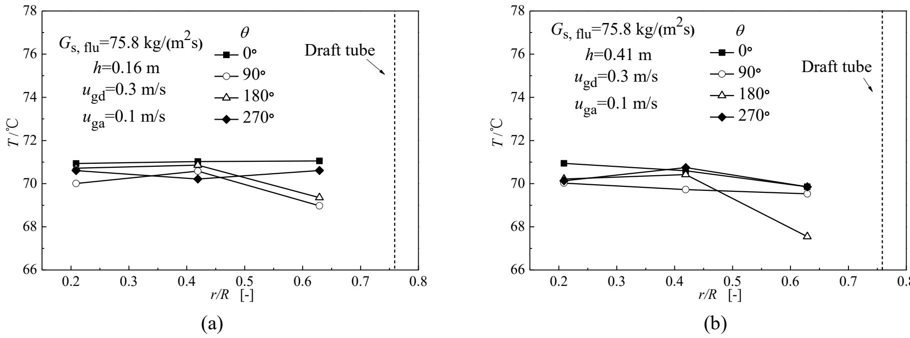

Fig. 5. The temperature distribution in draft tube zone

Fig. 6 reveals the temperature distribution in the slot zone. Compared with that in the lower cross-section (Fig.6 (a)), the temperature distribution in the higher cross-section (Fig.6 (b)) seems flat. Because in the slot zone, a part of particles flowed horizontally into the annulus zone through the shots, which was also called sub-circulation. It seems that the sub-circulation strongly promoted the radial particles mixing.

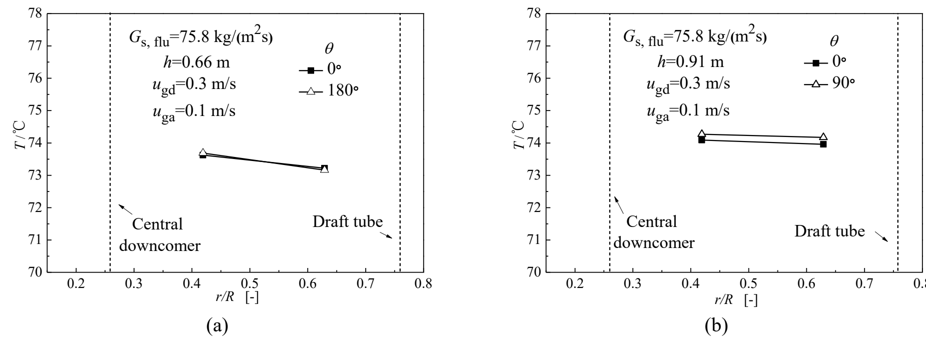

Fig. 6. The temperature distribution in slot zone

Fig. 7 shows the temperature distribution in the gas-solid separation zone. As shown in Fig.1, there exists radial flow of particles in this zone. The temperature in the center section ($0<r/R<0.63$) seems close, but in the section out of the center section temperature decreases. It suggests that the radial particle flow is not strong enough to achieve uniform mixing across the whole section. It is found that the temperature difference become small when the superficial gas velocity in the draft tube increased.

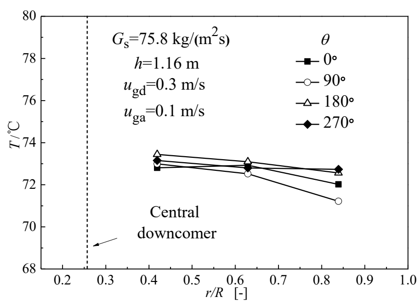

Fig. 7. The temperature distribution in gas-solid separation zone

The temperature distribution in bottom zone is shown in Fig. 8. The temperature seems uniform and consistent in the section of $0<r/R<0.65$, indicating that excellent fluidization quality and strong radial particle migration significantly enhanced the particle mixing. While in the section below the annulus, the temperature decreases, probably because the superficial gas velocity u_{ga} is only 0.1 m/s and the fluidization quality is poor.

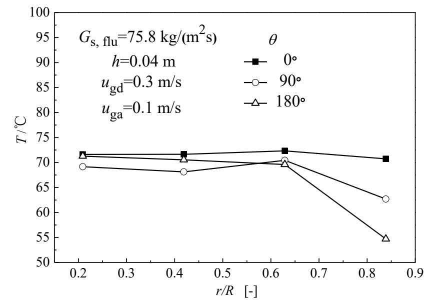

Fig. 8. The temperature distribution in bottom zone

3.2 Mixing uniformity

In order to quantitatively evaluate the mixing characteristics of the cold and hot particles in the bed, the present work used a mixing index I_M which was defined as follows (Fushimi et al., 2012).

$$T_i' = \left(\frac{T_i - T_c}{T_h - T_c}\right) \tag{1}$$

$$I_M = 1 - \frac{\sigma_p}{\sigma_0} \tag{2}$$

$$\sigma_0^2 = \overline{T'}(1 - \overline{T'}) \tag{3}$$

$$\sigma_p^2 = \frac{1}{N}\sum_1^N (T_i' - \overline{T'})^2 \tag{4}$$

$$\overline{T'} = \frac{1}{N}\sum_1^N T_i' \tag{5}$$

Here, T_i is the transient temperature in the bed; T_c is the temperature of cold particles; T_h is the temperature of hot particles; and T_i' represents the dimensionless temperature. I_M represents the mixing index; σ_0 is the standard deviation of the dimensionless temperature when the hot and cold particles are completely separated; σ_p is standard deviation of the dimensionless temperature; N is the quantity of the measuring point on the cross-section; $\overline{T'}$ represents the average dimensionless temperature on the cross-section.

When the mixing index I_M is equal to zero, it means that cold and hot particles do not mix completely. When I_M equals to 1, it indicates that cold and hot particles completely mix each other. Thus, the closer the I_M is to 1, the better the mixing of cold and hot particles is.

3.2.1 The mixing index I_M in the draft tube

The distribution of the mixing index in the draft tube is shown in Fig. 9. It is seen that the mixing index is quite small in the pre-mixing zone (h=1.5 m) where hot and cold particles were introduced, because the residence time of particles is not long enough for well mixing. In the MICFB section, particle mixing seems improved. In the bottom zone (h=0.04 m), particles are not well fluidized in the section below the annulus, leading to non-uniform particle mixing across the whole cross-section. But I_M significantly increases at h=0.41 m, where strong mixing occurs between hot particles from downcomer and particles in the draft tube. Compared with that at h=0.66 m, I_M decreases at h=0.91 m where four slots were opened. Because only in the vicinity of slots, particle radial flow and lateral mixing were enhanced, which led to non-uniform particle mixing in the whole cross-section. This suggests that a gap instead of few slots may facilitate a uniform particle mixing.

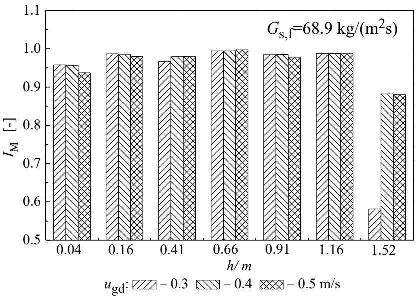

(a)

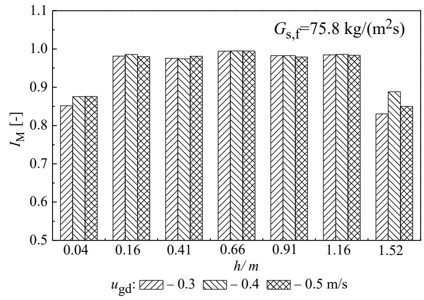

(b)

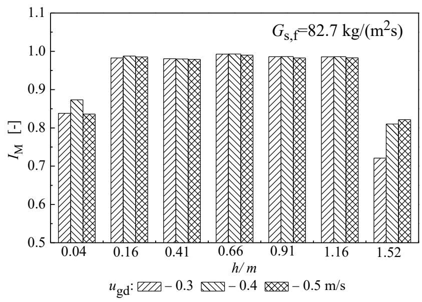

(c)

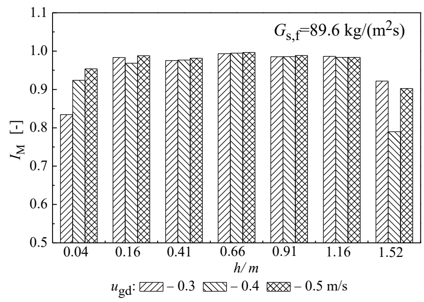

(d)

4. Conclusion

An ICFB mixer with a modified draft tube was proposed in this paper in order to improve the radial particle mixing. The mixing characteristics were investigated using thermal particle tracking technology. It is found that in the draft tube, the temperature seemed more uniform in the center than near the wall and the particles horizontal flow through the slots effectively promoted the radial mixing. The mixing index was over 0.97 in the draft tube. As the particles didn't fluidize well near the bottom of the annulus, the mixing index was as low as 0.65 in the annulus. The mixing performance was slightly changed with mass flux, while improved in the annulus with superficial gas velocity.

Notation

$G_{s,flu}$	mass flux, kg/(m^{3}s)	h	height, m
I_M	mixing index, [-]	N	quantity of the measuring point on the cross-section, [-]
r/R	dimensionless radius, [-]	T	temperature, ℃
$\overline{T'}$	average dimensionless temperature, [-]	T_c	temperature of the cold particles, ℃
T_h	temperature of the hot particles, ℃	T_i	transient temperature, ℃
T_i'	dimensionless temperature, [-]	u_{ga}	superficial gas velocity in the annulus, m/s
u_{gd}	superficial gas velocity in the draft tube, m/s	θ	angle, (°)
σ_0	standard deviation of the dimensionless temperature when the hot and cold particles are completely separated, [-]	σ_p	standard deviation of the dimensionless temperature, [-]

References

Fang, M., Luo, K., Yang, S., Zhang, K., Fan, J. 2013. Computational Fluid Dynamics-Discrete Element Method Investigation of Solid Mixing Characteristics in an Internally Circulating Fluidized Bed. Industrial & Engineering Chemistry Research 52, 7556-7568.

Fushimi, C., Guan, G., Nakamura, Y., Ishizuka, M., Tsutsumi, A., Suzuki, Y., Cheng, Y., Lim, E., Wang, C. 2012. Mixing behaviors of cold-hot particles in the downer of a triple-bed combined circulating fluidized bed. Powder Technology 221, 70-79.

Liu, M., Xie, J., Meng, Z., Lu, C. 2015. Hydrodynamic Characteristics and Mixing Characteristics of a New Type Particle Mixer. Journal of Chemical Engineering of Japan 48, 564-574.

Westphalen, D., Glicksman, L. 1995. Lateral solid mixing measurements in circulating fluidized beds. Powder Technology 82, 153-167.

Yang, S., Luo, K., Fang, M., Fan, J., Cen, K. 2014. Discrete Element Study of Solid Mixing Behavior with Temperature Difference in Three-Dimensional Bubbling Fluidized Bed. Industrial & Engineering Chemistry Research 53, 7043-7055.